large to be comfortably spanned by this ligand.

Conclusions

The use of 2-pyridyldiphenylphosphine as a bridging ligand in binuclear rhodium complexes containing a dimetalated olefin results in addition of carbon monoxide in terminal positions rather than in eventual insertion into the metal–metal bond to form a carbonyl-bridged species as occurs in the analogous DPM-bridged species. This is attributed to the shorter bite and greater rigidity of 2-pyridyldiphenylphosphine which prevents the rhodium atoms from separating enough to accommodate a bridging carbonyl ligand. Attempts to form iridium dimers bridged by this ligand appeared to succeed but were difficult, and the nature of the product could not be confirmed with certainty. Mixed rhodium–iridium dimers could not be prepared, presumably due to the greater stability of the dirhodium complex. The proposed structures and chemistry of DPM-bridged rhodium–iridium dimers containing a dimetalated olefin are a combination of those found previously for the homometallic counterparts. Interestingly, they show a much greater mobility of the carbonyl ligands than do either of these counterparts.

Acknowledgment. This research was primarily supported by the Chemistry Department of Tulane University. Partial support by the Gulf Oil Foundation is also gratefully acknowledged. We thank Professor Max Roundhill for helpful discussion and suggestions.

Registry No. 1, 100815-00-7; **2**, 100815-01-8; **3**, 100815-02-9; **4a**, 100815-03-0; **4b**, 101141-33-7; **5a**, 100815-04-1; **5b**, 101053-44-5; **6**, 100815-06-3; **7**, 100815-08-5; **8**, 100815-09-6; **9**, 100815-10-9; **10a**, 100815-11-0; **10b**, 100896-61-5; **11**, 100815-12-1; **12**, 100857-91-8; **13**, 100815-14-3; **14**, 100815-16-5; **16a**, 100815-17-6; **16b**, 100896-62-6; **16c**, 100815-18-7; $Rh_2Cl_2(\mu\text{-CO})(Ph_2Ppy)_2$, 75361-61-4; $Pd_2Cl_2(Ph_2Ppy)_2$, 78055-58-0; $PtBr_2(Ph_2Ppy)_2$, 84074-40-8; $Bu_4N[Ir(CO)_2Br_2]$, 73190-78-0; $[RhIr(CO)_2(\mu\text{-CO})Cl(DPM)_2]Cl$, 87482-56-2; $Ir(CO)_2Cl(p\text{-toluidine})$, 14243-22-2; $Ir_2Cl_2(c\text{-}C_8H_{14})_4$, 12246-51-4; Rh, 7440-16-6; Ir, 7439-88-5; Pt, 7440-06-4; dimethyl acetylenedicarboxylate, 762-42-5; heafluorobut-2-yne, 692-50-2; methyl propiolate, 922-67-8.

Reduction of Metal Carbonyls via Electron Transfer. Formation and Chain Decomposition of Formylmetal Intermediates

B. A. Narayanan, C. Amatore,[1] and J. K. Kochi*

Department of Chemistry, University of Houston, University Park, Houston, Texas 77004

Received July 30, 1985

Electron transfer to metal carbonyls such as $Cr(CO)_6$ and $Fe(CO)_5$ affords the corresponding 19-electron anion radicals which undergo facile hydrogen atom transfer with trialkyltin hydrides. The yields of the resultant formylmetal carbonyls are limited by a radical-chain decomposition, the mechanism of which is established by a detailed study of the formyldirhenate complex $(OC)_5ReRe(CO)_4CHO^-Bu_4N^+$ (IV). The chain process in Scheme I leading to the hydridodirhenate V is induced either thermally by azo initiator or photochemically with light of $\lambda > 400$ nm. High kinetic chain lengths and quantum yields of >300 are measured. Reductive methods involving initiation at an electrode surface or with sodium anthracene also promote the chain decomposition, but the turnover numbers are limited. Detailed kinetics analysis of the cyclic voltammetric data reveals the presence of two mechanistic pathways—one involving a radical-chain process (Scheme I) and the other an electron-transfer process (Scheme II). The radical-chain process for the decomposition of formylmetals is retarded by hydrogen atom donors. The latter is shown by the unusual stabilization of a variety of formylmetal species that are otherwise quite transient. Synthesis and decomposition of formylmetals by homolytic mechanisms involving facile hydrogen atom transfers are thus microscopically related processes.

Introduction

Current interest in metal carbonyls derives from their critical involvement in the industrially important catalytic reduction of carbon monoxide.[2,3] As part of our interest in organometallic electrochemistry, we recently found a series of facile homolytic reactions accompanying the one-electron oxidation and reduction of metal carbonyls.[4,5] Indeed the possibility of paramagnetic carbonylmetals participating as reactive intermediates in the catalytic CO reduction and Fischer–Tropsch synthesis has intrigued us for some time.[6] Since metal catalysis of carbon monoxide fixation has recently centered around formylmetal complexes as one of the prime intermediates along the reaction pathways,[7-9] we wish to focus on the production of this

(1) Present address: Laboratoire de Chimie, École Normale Supérieure, Paris, France 75231.

(2) (a) Wender, I.; Pino, P., Eds. "Organic Synthesis via Metal Carbonyls", Wiley: New York, (i) 1968; Vol. 1, (ii) **1976**; Vol. 2. (b) Henrici-Olive, G.; Olive, S. "The Chemistry of the Catalyzed Hydrogenation of Carbon Monoxide", Springer-Verlag: New York, 1984. (c) Masters, C. "Homogeneous Transition-Metal Catalysis"; Wiley: New York, **1980**.

(3) (a) Herman, R. G., Ed. "Catalytic Conversions of Synthesis Gas and Alcohols to Chemicals"; Plenum Press: New York, 1984. (b) *ACS Symp. Ser.* **1981**, *No. 152* and references therein. (c) Sheldon, R. A. "Chemicals from Synthesis Gas"; D. Reidel: Dordrecht, 1983.

(4) (a) Hershberger, J. W.; Klingler, R. J.; Kochi, J. K. *J. Am. Chem. Soc.* **1982**, *104*, 3034; **1983**, *105*, 61. (b) Hershberger, J. W.; Amatore, C.; Kochi, J. K. *J. Organomet. Chem.* **1983**, *250*, 345.

(5) (a) Narayanan, B. A.; Amatore, C.; Kochi, J. K. *J. Chem. Soc., Chem. Commun.* **1983**, 397. (b) Zizelman, P. M.; Amatore, C.; Kochi, J. K. *J. Am. Chem. Soc.* **1984**, *106*, 3771.

(6) Klingler, R. J.; Huffman, J. C.; Kochi, J. K. *Inorg. Chem.* **1981**, *20*, 34.

(7) (a) Olive, G. H.; Olive, S. *Angew. Chem., Int. Ed. Engl.* **1976**, *15*, 136. (b) Muetterties, E. L.; Stein, J. *Chem. Rev.* **1979**, *79*, 479. (c) Masters, C. *Adv. Organomet. Chem.* **1979**, *17*, 61. (d) Fahey, D. R. *J. Am. Chem. Soc.* **1981**, *103*, 136.

0276-7333/86/2305-0926$01.50/0

Table I. Electroreduction of Metal Carbonyls in the Presence of Tri-*n*-butyltin Hydride[a]

metal carbonyl	Bu_3SnH,[b] equiv	Q,[c] C	products
$Cr(CO)_6$	0	1.15	$Cr_2(CO)_{10}^{2-}$ [d]
$Cr(CO)_6$	5	1.07	$Cr(CO)_5CHO^-$ [e]
$Fe(CO)_5$	0	1.12	$Fe_2(CO)_8^{2-}$ [f]
$Fe(CO)_5$	5	1.08	$Fe(CO)_4CHO^-$ [g]
$Mn(CO)_4(PPh_3)_2^+PF_6^-$	0	1.40	$Mn(CO)_4PPh_3^-$ [h]
$Mn(CO)_4(PPh_3)_2^+PF_6^-$	5	1.10	$CH_3Mn(L)_x$ [i]

[a] Electroreductions were carried out under galvanostatic conditions (10^4 μA) using 5×10^{-2} M metal carbonyl in tetrahydrofuran containing 0.2 M tetra-*n*-butylammonium perchlorate. [b] Molar equivalent added relative to metal carbonyl. [c] Total charge passed per equivalent of metal carbonyl. [d] Identified by its characteristic[11] IR bands at 1905 and 1870 cm^{-1}. [e] Identified by its ^1H NMR resonance at δ 15.2 and IR band at 1595 cm^{-1} (–CHO).[13] Yield of 17% based on ^1H NMR analysis relative to *p*-dimethoxybenzene internal standard. [f] Identified by its characteristic[16] IR bands at 1920 and 1850 cm^{-1}. [g] Identified by its ^1H NMR resonance at δ 14.9 and IR band at 1602 cm^{-1} (–CHO).[17] Formed in 33% based on ^1H NMR analysis relative to *p*-dimethoxybenzene internal standard. [h] Identified by its characteristic[21] IR bands at 1940, 1850, and 1810 cm^{-1}. Minor amounts of $HMn(CO)_3(PPh_3)_2$ [^1H NMR δ –6.87 (d, J = 33 Hz) also formed]. [i] Uncharacterized crystalline methylmanganese complex showing an unresolved band at δ 0.13 (CH_3) similar to thatt (δ –0.30) of authentic $CH_3Mn(CO)_4PPh_3$. Minor amounts of $HMn(CO)_3(PPh_3)_2$ also formed.

crucial intermediate from metal carbonyls.[10] Such a demonstration is followed in this report by the delineation of efficient homolytic pathways for the subsequent rearrangement of formylmetal complexes to their hydridometal counterparts.

Results and Discussion

I. Formylmetal Complexes from the Electroreduction of Metal Carbonyls. Previous studies have established the electroreduction of chromium hexacarbonyl to produce the 17-electron radical anion $Cr(CO)_5^-\cdot$ which is subsequently dimerized in high yields,[11] i.e., eq 1. We

$$Cr(CO)_6 \xrightarrow{+e} Cr(CO)_6^-\cdot \xrightarrow{-CO} {}^1/_2Cr_2(CO)_{10}^{2-} \quad (1)$$

find that the 19-electron intermediate in eq 1 can be intercepted by efficient hydrogen atom donors.[12] Thus when the same electroreduction is carried out in the presence of tri-*n*-butyltin hydride, the known[13] formylchromium carbonyl $Cr(CO)_5CHO^-$ (I) is formed in ~20% yields. Similarly the use of tri-*n*-butyltin deuteride leads to the deuteriated formyl species $Cr(CO)_5CDO^-$, which establishes direct hydrogen atom transfer by a process such as eq 2.

$$Cr(CO)_6^-\cdot + Bu_3SnH \rightarrow \underset{\text{I}}{Cr(CO)_5CHO^-\cdot} \text{ etc.} \quad (2)$$

We believe that the homolytic trapping of $Cr(CO)_6^-\cdot$ in eq 2 is complete, being faster than the loss of CO and dimerization in eq 1, since none of the dimeric $Cr_2(CO)_{10}^{2-}$

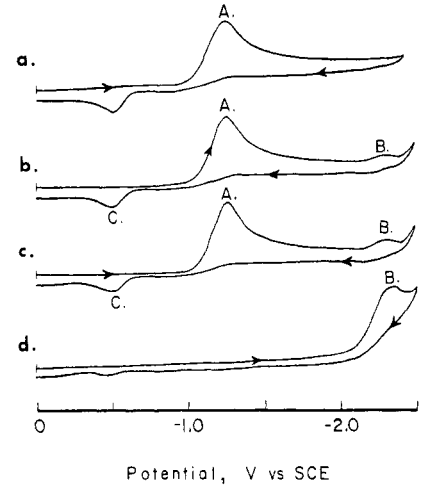

Figure 1. Initial negative scan cyclic voltammogram of 5×10^{-3} M $Mn(CO)_4(PPh_3)_2^+PF_6^-$ in tetrahydrofuran containing 0.1 M tetra-*n*-butylammonium perchlorate at a scan rate of 500 mV s^{-1}: (a) no Bu_3SnH; (b) 2.0×10^{-2} M Bu_3SnH; (c) 8×10^{-2} M Bu_3SnH. The cyclic voltammogram of 5×10^{-3} M $Mn(CO)_3(PPh_3)_2CHO$ under the same conditions is shown in (d).

was observed. Furthermore the NMR analysis of the electrolysis mixture indicated that the formyl species I is reduced to the hydroxymethyl moiety (vide infra) together with other products, which account for its less than quantitative yields in Table I.[14]

The initial electroreduction of iron pentacarbonyl is a one-electron process like that of chromium hexacarbonyl. Furthermore, it affords the dimeric $Fe_2(CO)_8^{2-}$ by a sequence of reactions akin to that described in eq 1.[16] Analogously, we find the 19-electron intermediate $Fe(CO)_5^-\cdot$ to be intercepted by tri-*n*-butyltin hydride to afford the well-known[17] formyliron carbonyl $Fe(CO)_4CHO^-$ (II) in 15–30% yields. Under these conditions, none of the dimeric $Fe_2(CO)_8^{2-}$ was observed.

$$Fe(CO)_5 + e \rightarrow Fe(CO)_5^-\cdot \xrightarrow{Bu_3SnH} \underset{\text{II}}{Fe(CO)_4CHO^-} \text{ etc.} \quad (3)$$

The chromium and iron carbonyls have served in this study as prototypes for homolytic hydrogen transfer to generate formylmetal species I and II, as in eq 2 and 3. As such, hydrogen atom transfer to the 19-electron carbonylmetal radical anions $Cr(CO)_6^-\cdot$ and $Fe(CO)_5^-\cdot$ must have occurred at rates which are competitive with other facile processes, such as the rapid loss of CO and dimerization.[18,19] Indeed the rapidity of hydrogen atom transfer can be independently demonstrated by transient electrochemical techniques. Thus Figure 1a shows the initial negative scan cyclic voltammogram of the cationic man-

(8) (a) Casey, C. P.; Neumann, S. M.; Andrews, M. A.; McAlister, D. R. *Pure Appl. Chem.* **1980**, *52*, 625. (b) Brady III, R. C.; Pettit, R. *J. Am. Chem. Soc.* **1981**, *103*, 1287.

(9) For a review see: Gladysz, J. A. *Adv. Organomet. Chem.* **1982**, *20*, 1.

(10) (a) Hydride transfer to metal carbonyls from various types of borohydrides and related reducing agents is usually the method of choice for the synthesis of formylmetal complexes.[3] (b) For a preliminary communication see: Narayanan, B. A.; Kochi, J. K. *J. Organomet. Chem.* **1984**, *272*, C49.

(11) (a) Dessy, R. E.; Stary, F. E.; King, R. B.; Waldrop, M. *J. Am. Chem. Soc.* **1966**, *88*, 471. (b) Pickett, C. J.; Pletcher, D. *J. Chem. Soc., Dalton Trans.* **1975**, 879; **1976**, 749. (c) Seurat, A.; Lemoine, P.; Gross, M. *Electrochim. Acta* **1978**, *23*, 1219.

(12) See, e.g.: Lusztyk, J.; Lusztyk, E.; Maillard, B.; Lunazzi, L.; Ingold, K. U. *J. Am. Chem. Soc.* **1983**, *105*, 4475.

(13) Casey, C. P.; Neumann, S. M. *J. Am. Chem. Soc.* **1976**, *98*, 5395.

(14) For example, in the ^2H NMR spectrum of the reaction mixture from the reduction of $Cr(CO)_6$ in the presence of Bu_3SnD, a strong resonance at δ 3.7 for the $HOCD_2$ group[15] was observed in addition to resonances at δ 8.8 (aldehydic), 15.2 (formyl), and –7.0 (hydride).

(15) Cf: Casey, C. P.; Neumann, S. M.; Andrews, M. A.; McAlister, D. R., in ref 8a.

(16) See ref 11 and: (a) Bond, A. M.; Dawson, P. A.; Peake, B. M.; Robinson, B. H.; Simpson, J. *Inorg. Chem.* **1977**, *16*, 2199.

(17) Collman, J. P.; Winter, S. R. *J. Am. Chem. Soc.* **1973**, *95*, 4089.

(18) For the intermediacy of $Fe(CO)_5^-\cdot$, see the ESR spectrum of species trapped in a single crystal of $Cr(CO)_6$. Fairhurst, S. A.; Morton, J. R.; Preston, K. F. *J. Chem. Phys.* **1982**, *77*, 5872. For some other 19-electron metal carbonyls, see also: Goldman, A. S.; Tyler, D. R. *J. Am. Chem. Soc.* **1984**, *106*, 4066. Stiegman, A. E.; Tyler, D. R. *Coord. Chem. Rev.* **1985**, *63*, 217.

(19) Although we favor the trapping of the 19-electron metal carbonyl radicals as in eq 2 and 3, we are unable to prove it solely on the basis of the product studies reported herein. Thus the less than quantitative yields of the formyl complexes and the identity of the tin-derived product do leave open the question of alternative pathways for their formation.

ganese carbonyl $Mn(CO)_4(PPh_3)_2^+$. The irreversible cathodic wave A with peak potential $E_p = -1.27$ V vs. SCE at 500 mV s^{-1} corresponds to a 1.1–1.5 e mol^{-1} process based on the calibration with a ferrocene standard. The addition of tri-*n*-butyltin hydride to the same solution prior to reduction leads to the appearance of a new cathodic wave B (Figure 1b, $E_p = -2.37$ V) which grows in importance as the amount of Bu_3SnH is increased (Figure 1c). The new cathodic wave B can be readily assigned to the neutral formyl complex $Mn(CO)_3(PPh_3)_2CHO$ (III), i.e., eq 4, by comparison with the cyclic voltammogram (Figure

$$Mn(CO)_4(PPh_3)_2^+ \xrightarrow{+e} Mn(CO)_4(PPh_3)_2\cdot \xrightarrow{Bu_3SnH} \underset{III}{Mn(CO)_3(PPh_3)_2CHO} \text{ etc.} \quad (4)$$

1d) of an authentic sample prepared by hydridic reduction of $Mn(CO)_4(PPh_3)_2^+$.[20] The appearance of the formyl species III during the time scale ($\sim 10^{-2}$ s) of the cyclic voltammetric scan thus supports the rapid rate of hydrogen atom transfer in eq 4.

In the absence of Bu_3SnH, the 19-electron radical $Mn(CO)_4(PPh_3)_2$ undergoes rapid transformation to the 17-electron species, followed by reduction to the anion,[21] i.e., eq 5. The carbonylmanganate ion is the principal product

$$Mn(CO)_4(PPh_3)_2\cdot \xrightarrow{-PPh_3} Mn(CO)_4PPh_3\cdot \xrightarrow{+e} Mn(CO)_4PPh_3^- \quad (5)$$

of the bulk electrolysis of $Mn(CO)_4(PPh_3)_2^+$ at a controlled potential which is slightly more negative than the CV wave A (i.e., −1.3 V). It appears in Figure 1 as the cyclic voltammetric wave C ($E_p = -0.5$ V), the peak current of which is shown to diminish with increasing amounts of the stannane hydrogen donor. In other words, the 19-electron carbonylmanganese radical under these conditions suffers phosphine loss which is competitive with hydrogen transfer, i.e., eq 6. By contrast, the bulk electroreduction

$$Mn(CO)_4(PPh_3)_2\cdot \begin{cases} \xrightarrow{Bu_3SnH} Mn(CO)_3(PPh_3)_2CHO \\ \xrightarrow{-PPh_3} Mn(CO)_4PPh_3\cdot \text{ etc.} \end{cases} \quad (6)$$

of the cationic carbonylmanganese complex $Mn(CO)_4(PPh_3)_2^+$ in the presence of tri-*n*-butyltin hydride affords no or little formyl complex III when carried out at a controlled potential of −1.3 V.[22] The discrepancy between the results of bulk electrolysis and cyclic voltammetry suggests that the formyl complex III is not stable, since the two electrochemical experiments differ principally only in the time scale of the experiment. Furthermore the somewhat limited yields of I and II in Table I together with the lability of carbonylmetal radicals (as in eq 6) do raise the question as to the fate of the formylmetals generally under homolytic conditions. In order to investigate this problem, we examined next the behavior of the formyldirhenate complex *cis*-$(OC)_5ReRe(CO)_4CHO^-Bu_4N^+$ (IV) owing to its known thermal stability.[24,25]

II. Transformation of Formylmetal Complexes by Chain Processes. The formyldirhenate complex IV remained unchanged in either tetrahydrofuran or acetonitrile solution (typically 10^{-1} M) for several days at 25 °C, provided the thoroughly degassed solutions were not exposed even to room light. However under certain conditions enumerated below, the formyldirhenate complex is efficiently transformed into the corresponding hydrido complex V.[26]

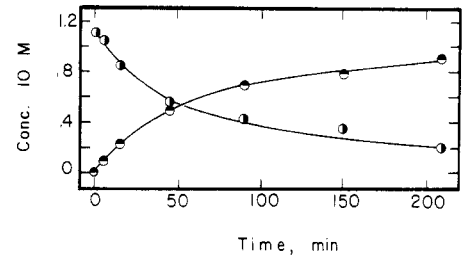

Figure 2. Conversion of the formyldirhenate IV (11×10^{-1} M) to the hydridodirhenate V by 10 mol % azobis(isobutyronitrile) in acetonitrile.

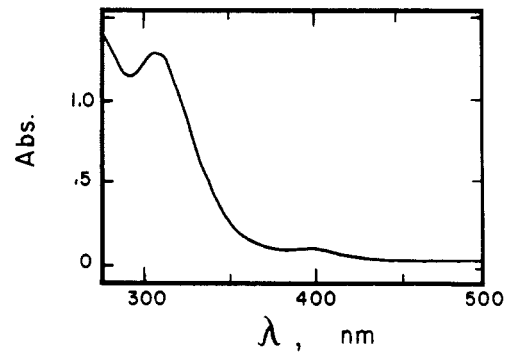

Figure 3. Absorption spectrum of $(OC)_5ReRe(CO)_4CHO^-Bu_4N^+$ (IV) (2.0×10^{-4} M) in tetrahydrofuran.

A. Thermal Initiation. Addition of only 10 mol % of the radical initiator azobis(isobutyronitrile) (AIBN) induced the transformation of IV to the corresponding hydride V, i.e., eq 7, in 90% yield within 4 h at 25 °C.[27]

$$\underset{IV}{(OC)_5ReRe(CO)_4CHO^-} \xrightarrow{[AIBN]} \underset{V}{(OC)_5ReRe(CO)_4H^-} + CO \quad (7)$$

The apparent half-life of the formyldirhenate complex IV is only 45 min in acetonitrile and 180 min in THF (see Figure 2). A turnover number of >500 was calculated from the known rate of AIBN homolysis under these conditions.[28] The radical-chain nature of the AIBN-induced transformation of IV to V was also revealed by the marked increase in the half-life $\tau_{1/2}$ in acetonitrile to more than 5 h by the presence of 1 equiv of dihydroanthracene.[29]

B. Actinic Initiation. The photochemically induced transformation[24,25] of the formyldirhenate IV to the corresponding hydridodirhenate V also proceeds via a radical-chain pathway. Thus the irradiation of 0.1 M IV in tetrahydrofuran with light either at $\lambda = 400 \pm 5$ nm using

(20) Tam, W.; Lin, G. Y.; Gladysz, J. A. *Organometallics* **1982**, *1*, 525.
(21) Hieber, W.; Gaulhaver, G.; Theubart. *Z. Naturforsch., B: Anorg. Chem., Org. Chem., Biochem., Biophys., Biol.* **1960**, *15B*, 326; *Z. Anorg. Allg. Chem.* **1962**, *314*, 125.
(22) Instead a yellow crystalline methylmanganese compound similar to $CH_3Mn(CO)_4PPh_3$ prepared independently[23] was isolated.
(23) Kraihanzel, C. S.; Maples, P. K. *Inorg. Chem.* **1968**, *7*, 1806.
(24) Casey, C. P.; Neumann, S. M. *J. Am. Chem. Soc.* **1978**, *100*, 2544.
(25) (a) Gladysz, J. A.; Tam, W. *J. Am. Chem. Soc.* **1978**, *100*, 2545. (b) Tam, W.; Marsi, M.; Gladysz, J. A. *Inorg. Chem.* **1983**, *22*, 1413.
(26) (a) For a preliminary communication, see: Narayanan, B. A.; Amatore, C.; Casey, C. P.; Kochi, J. K. *J. Am. Chem. Soc.* **1983**, *105*, 6351. (b) See also: Sumner, C. E.; Nelson, G. O. *J. Am. Chem. Soc.* **1984**, *106*, 432. Barratt, D. S.; Cole-Hamilton, D. J. *J. Chem. Soc., Chem. Commun.* **1985**, 458. Paonessa, R. S.; Thomas, N. C.; Halpern J. *J. Am. Chem. Soc.* **1985**, *107*, 4333.
(27) Disappearance of IV by its ^1H NMR spectrum at 16.1 ppm and appearance of V at −7.2 ppm, using *p*-di-*tert*-butylbenzene as internal standard.[24,25]
(28) Arnett, L. M. *J. Am. Chem. Soc.* **1952**, *74*, 2027.
(29) (a) Given arbitrarily as the time required for 50% decomposition under reaction conditions. (b) For dihydroanthracene as a hydrogen atom donor, see: Shine, H. J.; Waters, J. A.; Hoffman, D. M. *J. Am. Chem. Soc.* **1963**, *85*, 3613. Lockhart, T. P.; Comita, P. B.; Bergman, R. G. *J. Am. Chem. Soc.* **1981**, *103*, 4082.

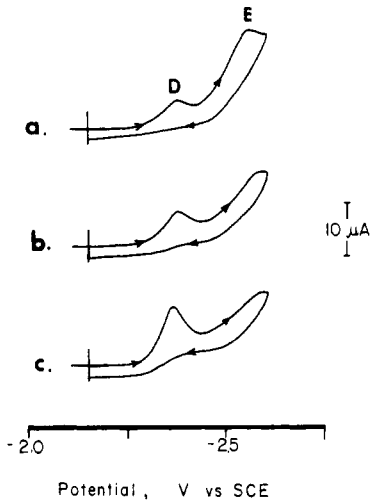

Figure 4. (a) Cyclic voltammogram of 5.0×10^{-3} M $(OC)_5ReRe(CO)_4CHO^-Bu_4N^+$ (IV) in acetonitrile containing 0.1 M TEAP at a scan rate of 200 mV s^{-1} at 25 °C. Cyclic voltammograms in (b) and (c) in the presence of 3 and 10 equiv of dihydroanthracene, respectively. D is the CV wave of IV and E that of the hydridodirhenate V.

an interference filter or at $\lambda > 400$ nm using sharp cutoff filters afforded the hydridodirhenate, i.e., eq 8, in 75%

$$(OC)_5ReRe(CO)_4CHO^- \xrightarrow{h\nu} (OC)_5ReRe(CO)_4H^- + CO \quad (8)$$

yield with $\tau_{1/2} \sim 30$ min. Importantly this value was markedly increased to $\tau_{1/2} > 10$ h in the presence of 1 equiv of dihydroanthracene. By the use of ferrioxalate actinometry,[30] the quantum yield for the photoinitiated conversion of IV to V was found to be $\Phi > 400$. The electronic absorption spectrum of formyldirhenate IV in Figure 3 has an absorption band at $\lambda_{max} = 310$ nm and a weak absorption at $\lambda_{max} = 400$ nm. Previous studies of the parent dirhenium decacarbonyl and its derivatives have shown that the lowest excited states in these complexes are reactive and lead to homolytic Re–Re cleavage,[31,32] e.g., eq 9.

$$(OC)_5ReRe(CO)_4CHO^- \xrightarrow{h\nu} Re(CO)_5\cdot + Re(CO)_4CHO^-\cdot \quad (9)$$

C. Electrochemical Initiation. Carbonylrhenium radicals can also be generated electrochemically.[26] For example, the galvanostatic reduction [E] of the formyldirhenate IV (2.0×10^{-2} M) in acetonitrile containing 0.1 M tetraethylammonium perchlorate (TEAP) as the supporting electrolyte consumed 0.035 F of charge/mol of IV to yield essentially quantitative yields of the hydridodirhenate V with the turnover number $\simeq$30, i.e., eq 10. The

$$\underset{IV}{(OC)_5ReRe(CO)_4CHO^-} \xrightarrow{[E]} \underset{V}{(OC)_5ReRe(CO)_4H^-} + CO \quad (10)$$

rapidity of the electrocatalytic process is revealed in the cyclic voltammogram in Figure 4a showing the cathodic current for the irreversible wave D at $E_p = -2.1$ V to be only one-fifth of that expected for a one-electron reduction (based on ferrocene calibration). It is accompanied by the simultaneous appearance of the hydridodirhenate V shown by the CV wave E at $E_p = -2.6$ V which was established by comparison with that of an authentic sample. The occurrence of a chain process for decomposition was also evident by the enhancement of the cathodic current for IV (and concomitant decrease in V) by incremental additions of dihydroanthracene as shown in parts b and c of Figure 4. Addition of larger amounts of dihydroanthracene led to a saturation effect, and the cathodic current for the CV wave of IV attained a maximum value which was only 60% of that expected from a one-electron reduction.

Scheme I

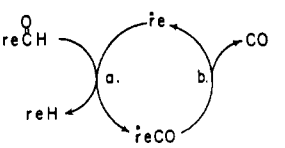

D. Reductive Initiation. The formyldirhenate IV was also found to undergo chain decomposition to its hydride V in the presence of small amounts of rather strong reducing agents [e]. For example, the addition of sodium anthracene (5 mol %) to a 0.1 M solution of IV in tetrahydrofuran was sufficient to effect conversion to V in 75% yield within 10 min at 25 °C.

$$\underset{IV}{(OC)_5ReRe(CO)_4CHO^-} \xrightarrow{[e]} \underset{V}{(OC)_5ReRe(CO)_4H^-} + CO \quad (11)$$

E. Chain Mechanism for the Formylmetal to Hydridometal Conversion. The long kinetic chain lengths together with the rate retardation by dihydroanthracene indicate an efficient conversion of IV to V by a radical chain process, the propagation sequence of which can be described in Scheme I, where re = $(OC)_5ReRe(CO)_4^-$. Precedent for both steps of the catalytic cycle derives from the studies of Brown and co-workers,[33] who demonstrated the ability of 17-electron carbonylrhenium radicals (i) to abstract hydrogen atoms from various donors as in step a and (ii) to exhibit the substitutional lability of carbonyl ligands as in step b.

Of the four methods of initiation described above, there exists a reasonable correspondence between two of them, namely, the thermal (AIBN) and photochemical processes for the conversion of the formyldirhenate IV into the corresponding hydride V. Thus both methods involve comparable turnover numbers of about >300, and retardation of the same magnitude by dihydroanthracene. Initiation of the chain process by hydrogen atom abstraction from the formylmetal complex is the common factor, i.e., eq 12. Initiation of the radical chain by AIBN

$$In\cdot + (OC)_5ReRe(CO)_4CHO^- \rightarrow In\text{–}H + (OC)_5ReRe(CO)_5^- \quad (12)$$

homolysis affords In· = $(CH_3)_2\dot{C}CN$, which is capable of hydrogen atom abstraction of formyl hydrogens,[34] as in eq 12. Similarly the photolysis of dirhenium carbonyls such as that described in eq 9 generates mononuclear carbo-

(30) Rabek, J. F. "Experimental Methods in Photochemistry and Photophysics"; Wiley: New York, 1982, p 944 ff.

(31) (a) Wrighton, M. S.; Ginley, D. S. *J. Am. Chem. Soc.* **1975**, *97*, 2065. (b) Ginley, D. S.; Wrighton, M. S. *J. Am. Chem. Soc.* **1975**, *97*, 4908. (c) Morse, D. L.; Wrighton, M. S. *J. Am. Chem. Soc.* **1976**, *98*, 3931.

(32) Cf. also: Levenson, R. A.; Gray, H. B.; Ceasar, G. P. *J. Am. Chem. Soc.* **1970**, *92*, 3653. Geoffroy, G. L.; Wrighton, M. S. "Organometallic Photochemistry"; Academic Press: New York, 1979, p 89 ff. Stolzenberg, A. M.; Muetterties, E. L. *J. Am. Chem. Soc.* **1983**, *105*, 822. Meckstroth, W. K.; Walters, R. T.; Waltz, W. L.; Wojcicki, A.; Dorfman, L. M. *Ibid.* **1982**, *104*, 1842. It is also possible that photochemical irradiation generates re· directly.

(33) Walker, H. W.; Rattinger, G. B.; Belford, R. L.; Brown, T. L., in footnote 18 and references therein. Note that mononuclear species such as $Re(CO)_5$· are unlikely to be important intermediates in the chain process, since products such as $HRe(CO)_5$ were not observed and high yields of $HRe_2(CO)_9^-$ were uniformly obtained.

(34) Nonhebel, D. C.; Walton, J. C. "Free-Radical Chemistry"; Cambridge University Press: New York, 1974. Compare also: Ingold, K. U. *Free Radicals* **1973**, *1*, 37.

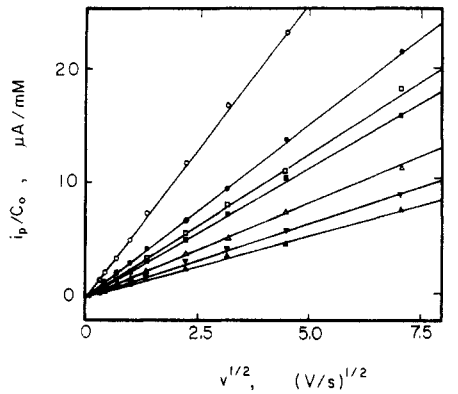

Figure 5. Variations in the CV peak current (normalized to the concentration of the reduction wave of IV) with the square root of the scan rate (in V s^{-1}). Comparison of anthracene (○) with IV at different concentrations: (●) 0.75 mM, (□) 1.10 mM, (■) 1.44 mM, (△) 2.70 mM, (▼) 4.73 mM, (▲) 9.7 mM (all in acetonitrile containing 0.1 M TEAP at 20 °C).

nylrhenium radicals particularly $Re(CO)_5$· which can also act as In· in eq 12.[35]

By contrast, the electrochemical initiation of the chain process is less efficient, the turnover numbers dropping to ~30 in the homogeneous experiments and to less than 4–5 in the transient experiments (compare the CV peak current in Figure 4). The marked contrast between the efficiencies of the radical initiation and the electrochemical initiation can be attributed to the reductive instability of the chain carriers reCO· and re· in Scheme I. In particular, these carbonylrhenium radicals are subject to further reduction to diamagnetic products,[36] e.g., eq 13 and 14, which

$$(OC)_5ReRe(CO)_4^- \xrightarrow{e} (OC)_5ReRe(CO)_4^{2-} \xrightarrow{H^+} (OC)_5ReRe(CO)_4H^- \quad (13)$$

$$\text{and/or } (OC)_5ReRe(CO)_5^- \xrightarrow{e} (OC)_5ReRe(CO)_5^{2-} \text{ etc.} \quad (14)$$

effectively interrupt the catalytic cycle. In other words, the electrochemical or reductive methods initiate the chain but simultaneously inhibit it, as has been shown in other systems.[37a] The overall result would lead to turnover numbers less than those obtained under nonreductive conditions.

A close scrutiny of the cyclic voltammograms in Figure 4 reveals the attainment of a limiting peak current which is less than that for a one-electron process even at very high concentrations of dihydroanthracene. This behavior suggests the presence of another chain process which is not inhibited by radical scavengers. Such an explanation is supported by the observation that dihydroanthracene is a less effective retarder in electrochemical methods compared to its effect on photochemical and thermal initiation. In order to examine the possibility, we undertook a thorough analysis of the dependence of the peak current i_p of the CV wave D in Figure 4 as a function of the scan rate v and the initial concentration C_0 of the formyldirhenate IV. Figure 5 presents the results of such an

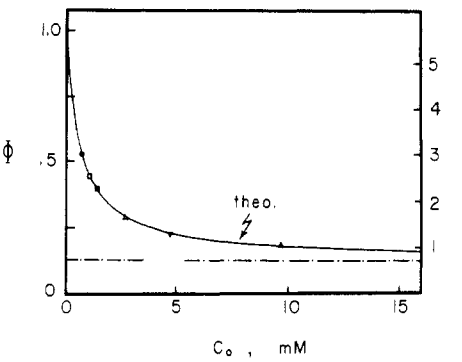

Figure 6. Variation of the slopes in Figure 5 (normalized to that taken as unity for anthracene) vs. the concentration of IV. The left scale indicates the absolute values of the slope in μA mM^{-1} $V^{-1/2}$ $s^{1/2}$.

analysis in the form of the variation of the normalized peak current i_p/C_0 with the scan rate. The results of the same analyses for anthracene (which represents a prototypical one-electron reversible CV wave[37b]) is included as a basis for comparison. Two conclusions can be drawn. First, the normalized peak current i_p/C_0 is proportional to the square root of the scan rate which indicates that the scan rate has no effect on the chain propagation. Second, the slopes in Figure 5 become smaller at increasing concentrations C_0, which indicates that chain propgation is more efficient at higher concentrations of formyldirhenate. This conclusion is more conveniently illustrated by plotting the variations of the normalized current function Φ with the initial concentration C_0, as shown in Figure 6.[38] Such a plot emphasizes the strong dependency of the efficiency of chain propagation on the initial concentration, especially at $C_0 < 3$ mM. The concentration levels off beyond $C_0 >$ 5 mM. These results are consistent with at least a pair of termination steps leading to deactivation of the chain process under reductive conditions. One of these termination steps can be largely overcome by simply increasing C_0, which suggests that it is a (first-order) process which competes with a second-order propagation reaction involving IV.[39] On the other hand, the saturation observed at the high range of concentrations suggests that a second termination step is also operating. Owing to its insensitivity to both C_0 and v, the second termination step is likely to involve a process with the same molecularity as that in the propagation cycle.

We present the catalytic mechanism in Scheme II to account for the alternative chain process involved in the conversion of IV to V under reductive conditions. Ac-

Scheme II

Initiation

$$(OC)_5ReRe(CO)_4CHO^- + e \rightarrow (OC)_5ReRe(CO)_4CHO)_4CHO^{2-}\cdot \quad (15)$$

Propagation

$$(OC)_5ReRe(CO)_4CHO^{2-}\cdot \xrightarrow{k_1} (OC)_5ReRe(CO)_4H^{2-}\cdot + CO \quad (16)$$

$$(OC)_5ReRe(CO)_4H^{2-}\cdot + (OC)_5ReRe(CO)_4CHO^- \xrightarrow{k_2} (OC)_5ReRe(CO)_4H^- + (OC)_5ReRe(CO)_4CHO^{2-}\cdot \quad (17)$$

(35) See ref 33 and: Byers, B. L.; Brown, T. L. *J. Am. Chem. Soc.* **1977**, *99*, 2527 for the homolytic reactivity of carbonylrhenium radicals.

(36) These carbonylrhenium radicals are electron-deficient relative to the dirhenate complexes IV and V, and the driving force for reduction should be correspondingly larger.

(37) (a) Cf.: Saveant, J. M. *Acc. Chem. Res.* **1980**, *13*, 323. See also: Amatore, C.; Pinson, J.; Saveant, J. M.; Thiebault, A. *J. Electroanal. Chem.* **1980**, *107*, 59, 75. (b) Cf., e.g.: Amatore, C.; Saveant, J. M. *J. Electroanal. Chem.* **1979**, *102*, 21. Amatore, C.; Saveant, J. M.; Thiebault, A. *J. Electroanal. Chem.* **1979**, *103*, 303. Zizelman, P. M.; Amatore, C.; Kochi, J. K., in ref 5b.

(38) The current function Φ is normalized both to C_0 and the san rate v as well as to anthracene owing to the difference in the nature of the waves (i.e., chemically irreversible for the formyl complex and chemically reversible for anthracene). This leads to the definition $\Phi = [i_p/(0.496C_0v^{1/2})]_{formyl}/[i_p/(0.446C_0v^{1/2})]_{anthracene}$.

(39) See, e.g.: Amatore, C.; Saveant, J. M. *J. Electroanal. Chem.* **1977**, *85*, 27.

cording to Scheme II, the initiation involves the reduction of IV to its dianion radical $(OC)_5ReRe(CO)_4CHO^{2-}\cdot$. The extrusion of CO from this 19-electron intermediate may involve one or more steps, but the exact sequence cannot be deduced from the data on hand.[40] On the basis of the dependence on C_0 and v, the pair of deactivating steps described above are attributed to the further evolution of the 19-electron intermediates $(OC)_5ReRe(CO)_4CHO^{2-}\cdot$ and $(OC)_5ReRe(CO)_4^{2-}\cdot$. These are associated with extrusion step (eq 16) and the electron-transfer step (eq 17), respectively. In order to test the validity of Scheme II, we derived the corresponding kinetics expression for the propagation sequence in eq 16 and 17 together with the initiation step (eq 15) and two first-order termination steps, as described in the Experimental Section. According to this formulation, the current function should vary according to eq 18, where k_1 and k_2 are the first-order and

$$\Phi = 1 - [0.227(k_2/k_4)C_0]/\{[1 + (k_3/k_1)][1 + 0.227(k_2/k_4)C_0]\} \quad (18)$$

second-order rate constants for eq 16 and 17, respectively, in the propagation cycle, and k_3 and k_4 are the pair of first-order termination rate constants. Indeed the fit of the experimental data to eq 18 is shown by the smooth curve drawn in Figure 6 using the rate constant ratios $k_2/k_4 = 6.8 \times 10^3$ M^{-1} and $k_3/k_1 = 0.15$. The electron-transfer mechanism based on Scheme II predicts a maximum turnover number of ~8 for the catalytic conversion of IV to V on the basis of these rate constant ratios. This value compares with the corresponding turnover number of >300 for the photochemical or thermal activation of the chain. Thus the electron-transfer propagation (Scheme II) will play a negligible role compared to the radical chain propagation (Scheme I) unless the latter is inhibited by processes such as those described in eq 13 and 14. Furthermore the experimental turnover number for electrochemical activation of 25–30 is significantly higher than that (8) predicted on the basis of Scheme II alone.[41] This indicates that the radical-chain propagation (Scheme I) is also initiated under reductive conditions. Such a reductive initiation relates to the cleavage previously observed with the parent dirhenium decacarbonyl,[42] viz., eq 19. The analogous cleavage of the Re–Re bond in IV leads

$$Re_2(CO)_{10} \xrightarrow{e} Re(CO)_5^- + Re(CO)_5\cdot \quad (19)$$

to carbonylrhenium radicals, i.e., eq 20, which like I· can

$$(OC)_5ReRe(CO)_4CHO^- \xrightarrow{e} \{Re(CO)_5\cdot + Re(CO)_4CHO^{2-}\} \text{ or } \{Re(CO)_5^- + Re(CO)_4CHO^-\cdot\} \quad (20)$$

enter the catalytic cycle in Scheme I. Such a reduction can occur heterogeneously at an electrode surface or homogeneously by reducing agents such as sodium anthracene. Evidence for the validity of the latter is obtained by comparison of the cyclic voltammetry of anthracene with that in the presence of IV. Figure 7a shows that the cyclic voltammogram of anthracene (An) is totally reversible (compare the cathodic and anodic peak currents) in

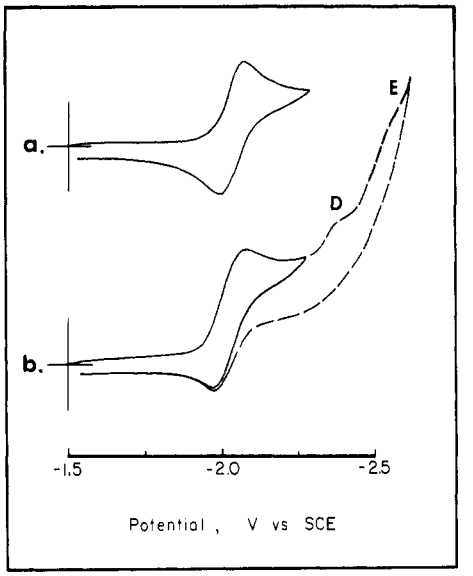

Figure 7. (a) Cyclic voltammogram of 5×10^{-3} M anthracene in acetonitrile containing 0.1 M TEAP at 200 mV s^{-1} and 20 °C. (b) Same but containing 5×10^{-4} M $(OC)_5ReRe(CO)_4CHO^-Bu_4N^+$. The dashed curve features the reduction peaks D and E for IV and V, respectively.

acetonitrile at a sweep rate of 200 mV s^{-1} at 20 °C. However when the formyldirhenate IV is present, there is an increase in the cathodic current together with a concomitant decrease in the anodic current (Figure 7b). Such a CV behavior is typical of a redox catalytic process of the following type[43]

$$An + e \rightarrow An^-\cdot \quad (21)$$

$$An^-\cdot + reCHO \rightleftharpoons An + reCHO^-\cdot \quad (22)$$

$$reCHO^-\cdot \rightarrow \ldots \quad (23)$$

According to this catalytic mechanism, the increase in the cathodic current in Figure 7b arises from the regeneration of anthracene by the electron-transfer step in eq 22. Likewise, the diminution in the anodic current derives from the consumption of the anion radical.

III. Stabilization of Formylmetal Complexes. Transient electrochemical techniques have allowed us to identify two principal pathways by which the formyldirhenate IV undergoes a catalytic chain decomposition. Since the functional transformation of a formyl group to a hydride ligand as in eq 7 also characterizes the decomposition of many other formylmetal species,[7-9] we inquire whether the same type of radical-chain mechanism outlined in Scheme I is a common factor in the apparent instabilities of this general class of organometallic intermediates. We initially focus our attention on the efficient radical-chain process under nonreducing conditions which is outlined in Scheme III, where MCHO and MH are generic representations of the formyl- and hydridometal species in the radical-chain process. Accordingly we have employed a variety of agents (i.e., retarders) in an attempt to intercept the chain-propagating radicals and thus prolong the half-life (stability) of the formylmetal complexes.[44]

Scheme III

$$MCHO + \cdot M \rightarrow \cdot MCO + MH \quad (24)$$

$$\cdot MCO \rightarrow CO + \cdot M \text{ etc.} \quad (25)$$

(40) Compare: (a) Fagan, P. J.; Moloy, K. G.; Marks, T. J. *J. Am. Chem. Soc.* **1981**, *103*, 6959. (b) Wayland, B. B.; Woods, B. A.; Pierce, R. *Ibid.* **1982**, *104*, 302. (c) Davies, S. G.; Simpson, S. J. *J. Organomet. Chem.* **1982**, *240*, C48.

(41) The difference can be viewed qualitatively in the following way. Cyclic voltammetry reflects electrochemistry under strong reductive conditions extant in the diffusion layer within a distance of 10–50 μm from the electrode. Bulk electrolysis includes this phenomenon plus any other processes, especially radical chains, which can occur outside the diffusion layer under nonreductive conditions.

(42) Lemoine, P.; Giraudeau, A.; Gross, M. *Electrochim. Acta* **1976**, *21*, 1.

(43) For the associated electrochemical kinetics, see: Nicholson, R. S.; Shain, I. *Anal. Chem.* **1964**, *36*, 706. See also: Amatore, C.; Oturan, M. A.; Pinson, J.; Saveant, J. M.; Thiebault, A. *J. Am. Chem. Soc.* **1984**, *106*, 6318.

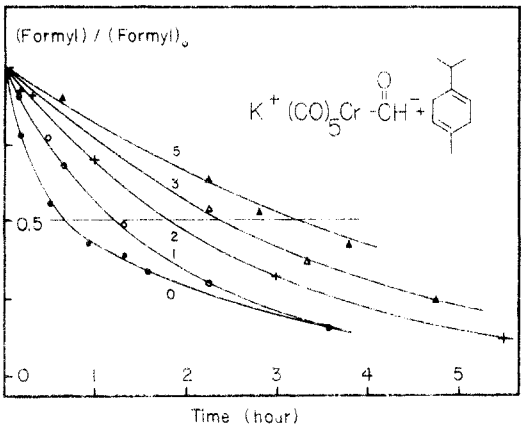

Figure 8. The effect of hydrogen atom donor on the decomposition of 1×10^{-1} M $Cr(CO)_5CHO^-$ in THF: (●) no additive, (○) 1, (+) 2, (△) 3, and (▲) 5 equiv of γ-terpinene.

Table II. Stabilization of the Formylchromium Complex $Cr(CO)_5CHO^-$ by Various Additives[a]

additive	n[b]	yield,[c] %	τ,[d] min	decomp products (% yield)
none		70	39	$Cr(CO)_5H^-$[e] (10), $(\mu\text{-}H)[Cr(CO)_5]_2^-$[f] (17)
γ-terpinene[g]	1	85	65	$Cr(CO)_5H^-$ (24)
	2	86	110	$Cr(CO)_5H^-$ (40)
	3	88	142	$Cr(CO)_5H^-$ (42)
	5	87	174	$Cr(CO)_5H^-$ (39)
dihydroanthracene[h]	1	85	80	$Cr(CO)_5H^-$ (15)
	2	86	123	$Cr(CO)_5H^-$ (34)
	3	85	139	$Cr(CO)_5H^-$ (42)
	5	88	160	$Cr(CO)_5H^-$ (41)
methoxy-1,4-cyclohexadiene[g]	1	82	104	$Cr(CO)_5H^-$ (24)
	2	85	118	$Cr(CO)_5H^-$ (37)
	3	88	122	$Cr(CO)_5H^-$ (42)
	5	88	138	$Cr(CO)_5H^-$ (43)

[a] All experiments were carried out in degassed, sealed Pyrex tubes. The formyl complex was generated in situ by the addition of a 10% molar excess of $K(i\text{-}PrO)_3BH$ (1 M solution in THF) to 1.0×10^{-1} M $Cr(CO)_6$ and the additive in THF. [b] Molar equivalents of additive present. [c] Yield of formylchromium complex $Cr(CO)_5CHO^-$ based on $Cr(CO)_6$ charged in the presence of additive. [d] Apparent halflife, see ref 29a. [e] Identified by its characteristic ^1H NMR resonance at δ −7.0.[46b] [f] Identified by its characteristic ^1H NMR resonance at δ −19.5.[46b] [g] *p*-Di-*tert*-butylbenzene used as the internal standard. [h] *p*-Dimethoxybenzene used as the internal standard.

We first examined the stabilization of the formylchromium complex $Cr(CO)_5CHO^-$ since it can be readily generated in >70% yield from chromium hexacarbonyl and a slight stoichiometric excess (10%) of potassium triisopropoxyborohydride $K(i\text{-}PrO)_3BH$ in tetraydrofuran (THF) solution.[13] Formed under these conditions, it decomposed with an apparent half-life of 39 min at 25 °C to afford the hydride $Cr(CO)_5H^-$ and the μ-hydride $(OC)_5CrHCr(CO)_5^-$ in 10% and 17% yields, respectively, among other unidentified products. However the halflife of $Cr(CO)_5CHO^-$ increased sharply in the presence of additives such a γ-terpinene (Figure 8), methoxy-1,4-cyclohexadiene, and dihydroanthracene, as listed in Table II.[45] Moreover, analysis of the decomposition products showed that the yield of the hydride $Cr(CO)_5H^-$ increased with increasing amounts of retarder. [By contrast, the formation of the μ-hydride $(OC)_5CrHCr(CO)_5^-$ was singularly inhibited by

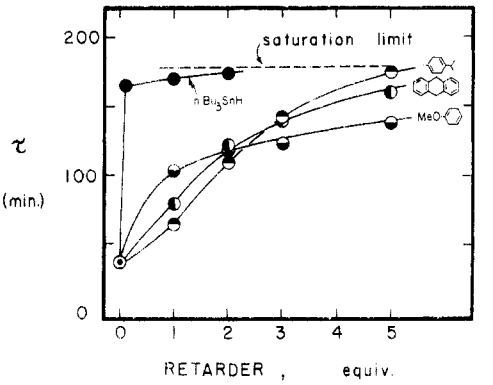

Figure 9. Variation of the stability (half-life) of the formylchromium complex $Cr(CO)_5CHO^-$ (1×10^{-1} M) in the presence of various amounts of retarders: γ-terpinene (⊖), dihydroanthracene (◐), methoxy-1,4-cyclohexadiene (⊖), tri-*n*-butyltin hydride (●) (molar equivalent relative to the formylmetal complex).

the presence of these retarders.[46]] Thus the conversion of the formylchromium complex $Cr(CO)_5CHO^-$ to the corresponding hydride species $Cr(CO)_5H^-$ is consistent with the radical-chain mechanism outlined in Scheme III. However, such a homolytic pathway cannot be the sole route by which the formyl complex decomposes for two reasons. First, the yield of $Cr(CO)_5H^-$ reaches a plateau of ~45% which is independent of the concentration and the structure of the retarder. Second, the half-life of the formylchromium complex also reaches a limiting value beyond which no added retarder has any effect. Indeed the results in Figure 9 show that the limiting values of the half-life are more or less the same for all retarders.[47] Thus we deduce that the plateau of $\tau_{1/2} \approx 170$ min represents a limit beyond which there exists only a nonradical-chain pathway for decomposition of the formyl complex.

The retarders listed in Table II have been identified as efficient hydrogen atom donors in organic homolytic systems.[48] Accordingly we next turned our attention to the trialkyltin hydrides which are known to be even more efficient as hydrogen atom donors.[12] Indeed we found that the maximum stabilization (i.e., $\tau_{1/2} \approx 165$ min) for the formylchromium complex $Cr(CO)_5CHO^-$ was readily attained with less than 0.1 equiv of $n\text{-}Bu_3SnH$ (see Table III). Further addition of the tin hydride had no effect on the half-life, in striking accord with the saturation limit described in Figure 9. Tributyltin hydride is also effective in the stabilization of a variety of other formylmetal complexes presented in Table III. Thus the formyltungsten complex $W(CO)_5CHO^-$ can be generated in 74% yield, and it has an apparent half-life of 16 min at 25 °C to afford the μ-hydride $(OC)_5WHW(CO)_5^-$ as the principal decomposition product. In the presence of $n\text{-}Bu_3SnH$, the half-life of $W(CO)_5CHO^-$ is prolonged substantially, and the principal product is the tungsten hydride $W(CO)_5H^-$, as given in Table III. Similarly the half-life of the mixed formylacetylrhenium complex[49] $CH_3CORe(CO)_4CHO^-$ can be increased from 8 to 78 min in the presence of 2 equiv of $n\text{-}Bu_3SnH$. Even haloformylrhenium complexes such as $BrRe(CO)_4CHO^-$ which is unstable at room temperature[50] could be stabilized by 2 equiv of $n\text{-}Bu_3SnH$ ($\tau_{1/2} \approx$

(44) For a preliminary report, see: Narayanan, B. A.; Amatore, C.; Kochi, J. K. *Organometallics* **1984**, *3*, 802.

(45) Typically, $Cr(CO)_5CHO^-$ is still present after 1 day in the presence of 3 equiv of additive, whereas it is completely gone within 2 h without additive.

(46) (a) Since it is known that the μ-hydride is formed from the monohydride on standing,[46b] the pronounced effect of the retarders suggests that this conversion may also proceed via radical intermediates. (b) Darensbourg, M. Y.; Deaton, J. C. *Inorg. Chem.* **1981**, *20*, 1644.

(47) The quality of the half-life values[29a] is sufficient to indicate a common convergence limit in Figure 1.

(48) See, e.g.: Kice, J. L. In "Free Radicals"; Wiley: New York, 1973; Vol. II, Chapter 24.

(49) Darst, K. P.; Lukehart, C. M. *J. Organomet. Chem.* **1979**, *171*, 65.

Table III. Stabilization of Various Formylmetal Complexes by *n*-Bu_3SnH[a]

formyl complex	yield,[b] %	Bu_3SnH, equiv	^1H NMR[c]	τ,[d] min	decomp products (% yield)
$Cr(CO)_5CHO^-K^+$	70		15.2	39	$Cr(CO)_5H^-$[e] (10), $(\mu\text{-}H)[Cr(CO)_5]_2^-$[f] (17)
$Cr(CO)_5CHO^-K^+$	92	0.1	15.1	165	$Cr(CO)_5H^-$ (16)
$Cr(CO)_5CHO^-K^+$	90	1	15.1	170	$Cr(CO)_5H^-$ (14)
$Cr(CO)_5CHO^-K^+$	86	2	15.1	172	$Cr(CO)_5H^-$ (35)
$W(CO)_5CHO^-K^+$	74		15.9	16	$(\mu\text{-}H)[W(CO)_5]_2^-$[g] (17)
$W(CO)_5CHO^-K^+$	76	1	15.8	28	$W(CO)_5H^-$[h] (50)
$W(CO)_5CHO^-K^+$	76	2	15.8	60	$W(CO)_5H^-$ (48)
$(CH_3CO)Re(CO)_4CHO^-K^+$	87	2	15.7	78	$(CH_3CO)Re(CO)_4H^-$[n,o] (32)
$Re(CO)_4BrCHO^-Li^+$[m]	58	1	14.95	130	*i*
$Mn(CO)_3(PPh_3)_2CHO$[j]	77	2	13.45	30	$HMn(CO)_3(PPh_3)_2$[k] (15)
$MO(CO)_5CHO^-K^+$[l]	40	2	15.4	<10	*i*
$Mn_2(CO)_9CHO^-Li^+$	p	2			*i*

[a] The formylmetal complexes were formed either by the addition of $K(i\text{-}PrO)_3BH$ (1 M in THF) or $Li(C_2H_5)_3BH$ (1 M THF) to a 1.0×10^{-1} M solution of the parent metal carbonyl and the appropriate amount of *n*-Bu_3SnH in THF. Experiments performed in degassed, sealed NMR tubes. [b] The yields refer to the conversion of the metal carbonyl to the formylmetal complex. [c] Formyl resonance relative to Me_4Si. [d] Apparent half-life, see ref 29a. [e] Identified by its characteristic ^1H NMR resonance δ −7.0.[46b] [f] Identified by its characteristic ^1H NMR resonance δ −19.5.[46b] [g] Identified by its characteristic ^1H NMR resonance δ −12.5.[46b] [h] Identified by its characteristic ^1H NMR resonance δ −4.5.[46b] [i] No hydride resonances could be observed between −0 and −30.0 ppm. [j] The formyl complex was formed by the addition of a slight excess of $Li(C_2H_5)_3BH$ (1 M in THF) to 2×10^{-2} M $Mn(CO)_4(PPh_3)_2^+PF_6^-$ in CH_2Cl_2. [k] Identified by its characteristic ^1H NMR spectrum (δ −7.2 (t, J = 33 Hz). [l] In the absence of *n*-Bu_3SnH, the formyl complex was formed in 17% yield. [m] In the absence of *n*-Bu_3SnH, $Re(CO)_5H$ (δ −5.2) was formed exclusively in 85% yield. [n] Identified by its characteristic ^1H NMR spectrum (δ −4.7).[49] [o] In the absence of Bu_3SnH, the hydride was formed in 94% yield. [p] Not stable at room temperature.

130 min at 25 °C). Likewise, the neutral formyl complex $Mn(CO)_3(PPh_3)_2CHO$,[51] which decomposes readily at 0 °C, could be seen at room temperature ($\tau_{1/2} \approx 30$ min) in the presence of 2 equiv of *n*-Bu_3SnH.

There are some formylmetal complexes such as $(OC)_5MnMn(CO)_4CHO^-$[52] and $Mo(CO)_5CHO^-$[13] whose stabilities are not noticeably affected by the presence of *n*-Bu_3SnH. Since these formyl complexes do not afford the corresponding hydrides as decomposition products, we tentatively infer that the radical-chain mechanism in Scheme III is mainly applicable to those formylmetal complexes which are readily converted to their hydride derivatives.

The existence of additional nonradical-chain pathways by which formylmetals can disappear may in part be related to the electron-transfer mechanism identified by transient electrochemical methods in Scheme II. If so, the divergent behavior of such formylmetal complexes as $(OC)_5MnMn(CO)_4CHO^-$ and $Mo(CO)_5CHO^-$ (vide supra) may be related to the ease by which they participate in electron-transfer processes. We believe that the contribution of electron-transfer and other molecular pathways[53] to the decomposition of the other formylmetal intermediates merits further delineation.[54]

Summary and Conclusions

Reduction of metal carbonyls such as $Cr(CO)_6$ and $Fe(CO)_5$ leads to their anion radicals as transient intermediates. These 19-electron species are trapped by hydrogen atom donors to afford the corresponding formylmetal complex. The two-step process is schematically represented as eq 26. The formylmetal in turn is subject to

$$MCO \xrightarrow{[e]} MCO^-\cdot \xrightarrow{[H]} MCHO^- \qquad (26)$$

chain decomposition leading to the corresponding hydridometal, i.e., eq 27.

$$MCHO \rightarrow MH + CO \qquad (27)$$

The detailed study of the formyl to hydridometal conversion with the formyldirhenate IV demonstrates that it is kinetically controlled, being considerably enhanced under radical (AIBN), photochemical, electrochemical, and reductive conditions. Under radical and photochemical conditions, the lifetime of the formylmetal decreases due to a radical-chain process outlined in Scheme I, in which the radicals re· and reCO· are the effective propagating species. Under electrochemical (cathodic) and reductive (sodium anthracene) conditions, these radicals are destroyed (eq 13 and 14), which results in the inhibition of the radical-chain process as shown by a decrease in the catalytic turnover numbers from >300 found in the radical and photochemical activations to 7–30 under reductive conditions. The formyl to hydridometal conversion, which is shown to be also activated under reducing conditions, is attributed to the participation of a second catalytic process which is modulated by electron transfer (Scheme II). In the case of formyldimetals such as $(OC)_5ReRe(CO)_4CHO^-$ (IV), the two processes are coupled as outlined in Scheme IV.

Scheme IV

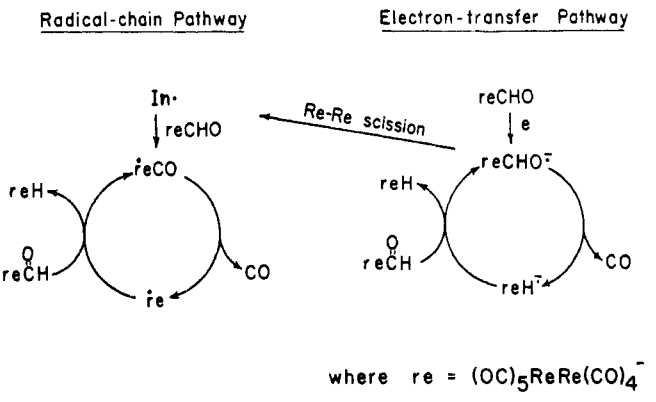

(50) See ref 49. Note that $BrRe(CO)_4CHO^-$ has been stabilized by the addition of LiBr. The decomposition products will be reported at a later time.

(51) Tam, W.; Lin, G. Y.; Gladysz, J. A., in ref 20.

(52) Tam, W.; Marsi, M.; Gladysz, J. A., in ref 25b.

(53) See, e.g., ref 8a and: Davies, S. G.; Hibberd, J.; Simpson, S. J. *J. Chem. Soc., Chem. Commun.* **1982**, 1404. Compare also: Lin, Y. C.; Milstein, D.; Wreford, S. S. *Organometallics* **1983**, *2*, 1461.

(54) Borohydrides and related hydridic reducing agents used in the synthesis of formylmetal complexes are known to participate in radical reactions.[55] Thus the values of τ observed in the absence of retarders may already represent partially retarded processes. If so, the actual radical chain process for formylmetal decomposition may be even more efficient than indicated by τ in the absence of retarder.

(55) See, e.g.: Ashby, E. C.; Goel, A. B.; DePriest, R. N.; Prasad, H. S. *J. Am. Chem. Soc.* **1981**, *103*, 973. Michaud, P.; Astruc, D.; Ammeter, J. H. *J. Am. Chem. Soc.* **1982**, *104*, 3755. Wagner, W. R.; Rastetter, W. H. *J. Org. Chem.* **1983**, *48*, 294. Baban, J. A.; Brand, J. C.; Roberts, B. P. *J. Chem. Soc., Chem. Commun.* **1983**, *315*. Beckwith, A. J.; Goh, S. H. *J. Chem. Soc., Chem. Commun.* **1983**, *905*. Chung, S. K. *J. Org. Chem.* **1980**, *45*, 3513, for some leading references.

The generality of the radical-chain process is demonstrated by the unusual stabilization by various hydrogen atom donors of a wide variety of otherwise transient formylmetal species. These hydrogen atom donors act by scavenging the effective propagating radicals in Scheme III. Thus hydrogen atom transfer in eq 24 and its microscopic reverse in eq 2 plays a critical role in the production and decomposition of the formylmetal intermediate during the reduction of metal carbonyls.

Experimental Section

Materials. The metal carbonyls $Cr(CO)_6$, $Mo(CO)_6$, $W(CO)_6$, and $Re_2(CO)_{10}$ from Pressure Chemicals were resublimed prior to use. $Fe(CO)_5$ was distilled in vacuo. $Re(CO)_5Br$,[56] CH_3CO-$Re(CO)_5$,[49] and $Mn(CO)_4(PPh_3)_2{}^+PF_6{}^-$[57] were synthesized from literature procedures. The formyldirhenate IV and the hydridodirhenate V were prepared as the tetra-*n*-butylammonium salts using the procedure described by Casey and Neumann.[24] Azobis(isobutyronitrile) (AIBN) and anthracene (Aldrich) were used without further purification. 9,10-Dihydroanthracene (Aldrich) was purified by column chromatography (silica gel, toluene) followed by recrystallization from toluene. It was stored under argon in the dark. 1,4-Dimethoxybenzene and γ-terpinene (Aldrich) were distilled from sodium and stored under argon. Potassium isopropoxyborohydride (1M in THF) and lithium triethylborohydride (1 M in THF) both from Aldrich were stored under argon and otherwise used as received. Tetraethylammonium perchlorate (G.F. Smith) was recrystallized from ethyl acetate and dried in vacuo for 24 h prior to use. Reagent grade acetonitrile (1 kg, Fisher) was repurified by first refluxing over $KMnO_4$ (15 g) and P_2O_5 (5 g) for $1^1/_2$ h. The mixture was filtered (liquid should be colorless), and diethylene triamine (6 g) was added. The mixture was distilled through a 20-plate Oldershaw column at high reflux ratios. The quality of the purified solvent was monitored by UV spectroscopy, and it showed less than 0.1 absorbance in a 1-cm cuvette at 200 nm. Tetrahydrofuran (Mallinckrodt, reagent grade) was distilled from sodium benzophenone and stored under argon. Sodium anthracene was prepared by dissolving anthracene (356 mg, 2 mmol) and sodium (46 mg, 2 mmol) in 50 mL of freshly distilled THF. The dark blue solution[58] was assayed (3.4×10^{-2} M) by quenching with O_2-free water and titration with standard hydrochloric acid.

Instrumental Methods. Electrochemistry was performed with a Princeton Applied Research Model 173 potentiostat/galvanostat equipped with a Model 176 current-to-voltage converter which provided a feedback compensation for ohmic drop between the working and reference electrodes. Bulk coulometry and cyclic voltammetry were performed in cells similar to the ones described previously.[4-6] UV/vis spectra were recorded on a Hewlett-Packard Model 8450A diode-array spectrometer. Photochemical irradiations were carried out with a 500-W xenon lamp using either an Interference filter (405 ± 5 nm, Edmund) or a Pyrex sharp cutoff filter (400 nm, Corning 3-74). The quantum yield were measured by ferrioxalate actinometry in the following way. Potassium ferrioxalate was prepared as the trihydrate,[59] and 0.889 mmol (490 mg) was dissolved in 3 mL of 0.1 N H_2SO_4. After irradiation, the solution was diluted 50-fold and treated with phenanthroline in an acetate buffer. The absorbance of the solution at 510 nm was compared with that of the unirradiated control. Under similar conditions, the formyldirhenate IV underwent 14% decomposition in 16 min, as analyzed by ^1H NMR spectrophotometry using *p*-di-*tert*-butylbenzene as an internal standard. Under these conditions the quantum yield was 335. ^1H NMR spectra were recorded either on a JEOL FX-90Q FT spectrometer or a Varian T60 NMR spectrometer. Infrared spectra were obtained on a Perkin-Elmer 298 spectrometer. All experiments were performed under an atmosphere of dry, prepurified nitrogen or argon in semidarkness, unless indicated otherwise.

Electroreduction of Metal Carbonyls. A solution of 5×10^{-2} M metal carbonyl in tetrahydrofuran containing 0.1 M tetraethylammonium perchlorate was reduced at a platinum electrode under galvanostatic conditions at 10^4 μA until slightly more than 1 electron mol^{-1} of charge was passed. The resulting solution was analyzed by either ^1H NMR spectroscopy by focussing on the characteristic formyl resonance or IR spectroscopy of the carbonyl ligands, as described in Table I. After the addition of 5 molar equiv of tri-*n*-butyltin hydride relative to the metal carbonyl, the experiment was repeated. Although no attempt was made to isolate the formylmetal complex, the formyliron carbonyl II was prepared by an independent procedure and obtained as a crystalline PPN salt.[60] Spectral comparisons established that it was formed as indicated in Table I.

Thermal Decomposition of $(OC)_5ReRe(CO)_4CHO^-Bu_4N^+$ (IV) in the Presence of AIBN. A thoroughly degassed solution of 10^{-1} M formyldirhenate IV in either THF or MeCN was kept at 25 °C and periodically analyzed by either ^1H NMR spectroscopy [δ 16.1 (CD_3CN)] or IR spectroscopy [2084 (w), 2066 (m), 2015 (s), 1979 (s), 1949(w), 1899(w), 1560 (m) cm^{-1}]. AIBN (2 mg, 10 mol %) was added to a solution of IV (100 mg, 0.112 mmol) in 0.6 mL of CD_3CN (containing a known amount of *p*-di-*tert*-butylbenzene) in a NMR tube. The solution was degassed by successive freeze–pump–thaw cycles and sealed in vacuo. The course of decomposition was followed by measuring the disappearance of the proton resonances at δ 16.1 and the simultaneous appearance of the hydrido resonance of the hydridodirhenate V [^1H NMR δ −7.2; IR 2078 (w), 2028 (m), 1972 (s), 1924 (m), 1888 (m) cm^{-1}]. The first-order rate constant for the decomposition of AIBN was calculated to be $k_1 = 10^{-7}$ s^{-1} at 20 °C from the relationship $\log k_1 = 7019T^{-1} + 17.807$, described by Arnett.[28] From the concentration of isobutyronitrile radicals, the lower limit for the turnover number was found to be >400. The experiments in THF and in the presence of dihydroanthracene were carried out in a similar manner.

Photochemical Decomposition of $(OC)_5ReRe(CO)_4CHO^-Bu_4N^+$. In a typical experiment a thoroughly degassed solution of IV (100 mg, 0.112 mmol) in 0.6 mL of THF with a known amount of *p*-di-*tert*-butylbenzene was sealed in a NMR tube in vacuo after successive freeze–pump–thaw cycles. The course of photolysis was followed by measuring the disappearance of the proton resonance at δ 16.1 and the concomitant appearance of the hydrido resonance at δ −7.2. A plot of the concentration of IV with time gave an apparent halflife of 30 min. The experiments in the presence of dihydroanthracene were carried out similarly. Quantum yields were determined by ferrioxalate actinometry (vide supra).

Electrochemical Decomposition of $(OC)_5ReRe(CO)_4CHO^-Bu_4N^+$ (IV). Formyldirhenate IV (100 mg, 0.112 mmol) was dissolved in 5 mL of acetonitrile containing 0.1 M TEAP. A constant cathodic current of ~1 mA was passed through the solution. The electrolysis was complete when the potential changed rather abruptly from −2.1 to −2.4 V. The catholyte was transferred to a Schlenk flask under an atmosphere of nitrogen and the solvent removed in vacuo. A known amount of *p*-di-*tert*-butylbenzene was added as an internal standard, and the resulting solution was analyzed by NMR spectroscopy using CD_3CN as the solvent. Yield of the hydridodirhenate V was ≃94%.

Decomposition of $(OC)_5ReRe(CO)_4CHO^-Bu_4N^+$ in the Presence of Sodium Anthracene. A 1.0-mL aliquot of 3.4×10^{-1} M sodium anthracene in THF was added to a solution of IV (300 mg, 0.336 mmol) in 4 mL of THF. After the solution was stirred for 10 min, the solvent was removed in vacuo and a known amount of *p*-di-*tert*-butylbenzene was added as an internal standard. ^1H NMR analysis showed a 75% conversion of IV to V.

Stabilization of Formylmetal Complexes. The formylmetal complexes were generated in situ by treating the appropriate metal carbonyl with a 10% molar excess of either potassium isoprop-

(56) (a) Abel, E. W.; Wilkinson, G. *J. Chem. Soc.* **1959**, 1501. (b) Hileman, J. C.; Huggins, D. K.; Kaesz, H. D. *Inorg. Chem.* **1962**, *1*, 933.
(57) Angelici, R. J.; Brink, R. W. *Inorg. Chem.* **1973**, *12*, 1067. Cf.: Paul, D. E.; Limkin, D.; Weismann, S. L. *J. Am. Chem. Soc.* **1956**, *78*, 116.
(58) Cf.: Paul, D. E.; Limkin, D.; Weismann, S. L. *J. Am. Chem. Soc.* **1956**, *78*, 116.
(59) Calvert, J. G.; Pitts, J. N., Jr. "Photochemistry"; Wiley: New York, **1966**; pp 784–5.
(60) Zizelman, P. M., unpublished work.

oxyborohydride or lithium triethylborohydride, as specified in Table III. The stability of such a solution was followed by ^1H NMR spectroscopy by measuring the disappearance of the characteristic formyl resonance in the ^1H NMR spectrum in a sealed tube in vacuo. The experiment was repeated with various hydrogen donors which were added to the preformed formylmetal complex prior to sealing the tube. The spectral characteristics are included in Tables II and III.

Derivation of the Current Function (eq 18) for Electron-Transfer Catalysis. Consider the mechanism in Scheme II and the pair of termination steps with first-order rate constants k_3 and k_4 for $reCHO^{-}\cdot$ and $reH^{-}\cdot$, respectively. Assuming steady-state kinetics for $reH^{-}\cdot$, it follows that[61]

$$k_1[reCHO^{-}\cdot] = (k_4 + k_2[reCHO])[reH^{-}\cdot] \quad (28)$$

Let $a = [reCHO]/C_0$, $b = [reCHO^{-}\cdot]/C_0$, $\lambda = k_1(RT/Fv)$, $\sigma = k_3/k_1$, $\rho = k_2C_0/k_4$, $\tau = t(Fv/RT)$, $y = x(Fv/DRT)^{1/2}$, and $\xi = -(F/RT)(E - E^\circ)$, where C_0 is the initial and bulk concentration of IV, t the elapsed time since the start of the CV scan, v the scan rate, x the distance from the electrode, D the average diffusion coefficient, E the electrode potential, and E° the standard reduction potential of IV. From Scheme II[37-39]

$$\frac{\partial a}{\partial \tau} = \frac{\partial^2 a}{\partial y^2} - \lambda[\rho a/(1 + \rho a)]b \quad (29)$$

$$\frac{\partial b}{\partial \tau} = \frac{\partial^2 b}{\partial y^2} - \lambda[\sigma + 1/(1 + \rho a)]b \quad (30)$$

associated with the following initial and boundary conditions:

$$\tau = 0 \text{ or } y \to \infty: \; a = 1, \; b = 0$$

$$\tau > 0, \; y = 0: \; a_0 = b_0 \exp(-\xi) \text{ and } (\partial a/\partial y)_0 + (\partial b/\partial y)_0 = 0$$

The current (i) variations with time or potential is given by $\psi = (\partial a/\partial y)_0 = -(\partial b/\partial y)_0$ as a function of τ or ξ with $\psi = i/\{(FSC_0)[(DFv)/(RT)]^{1/2}\}$, where S is the surface area of the electrode. Since the CV wave for IV is irreversible at all the scan rates investigated, the rate constants k_1 and k_3 are sufficiently large for pure kinetic conditions to apply to b. Thus IV exists only in a thin kinetic layer adjacent to the electrode such that for $0 \le y \le \mu$, $a \simeq a_0 \simeq a_\mu$, and $\partial b/\partial \tau \simeq 0$. Integration then yields $\psi = b_0[\lambda[\sigma + 1/(1 + \rho a_\mu)]]^{1/2}$ and $b = b_0 \exp\{-y(\lambda[\sigma + 1/(1 + a_\mu)])^{1/2}\}$which finally gives

$$a_\mu = \psi\{\lambda[\sigma + 1/(1 + \rho a_\mu)]^{-1/2} \exp(-\xi)\} \quad (31)$$

On the other hand, the integration of the sum of eq 29 and 30 inside the kinetic layer yields

$$(\partial a/\partial y)_\mu = \lambda(1 + \sigma)\int_0^\mu b \, dy = \Psi(1 + \sigma)/[\sigma + 1/(1 + \rho a_\mu)] \quad (32)$$

and outside the kinetic layer (i.e., $y > \mu$) $b = 0$, for which

$$a_\mu = 1 - \pi^{-1/2}\int_0^\tau (\partial a/\partial y)_\mu (\tau - n)^{-1/2} \, d\eta = 1 - I\Psi_\mu \quad (33)$$

The equation for the cyclic voltammogram can be obtained from eq 31–33 in the form of the variations of Ψ with τ and can be solved by numerical methods. However, we considered an approximate solution by making the following simplification. In the potential region where the CV wave is displayed, a_μ varies smoothly, and the combination of eq 31 and 33 into the form $\Psi_\mu = (\partial a/\partial y)_\mu$ and

$$1 - I\Psi_\mu = \Psi_\mu \exp(-\xi^*) \quad (34)$$

where $\xi^* = \xi + {}^1/_2 \ln\{\lambda(\sigma + 1)^2[\sigma + 1/[1 + \rho(1 - I\Psi_\mu^p)]\} \simeq \xi + cst$, where the superscript p indicated the peak value. The solution of eq 34 yields[62] $\Psi_\mu^p = 0.496$ and $a_\mu^p = (1 - I\Psi_\mu^p) \simeq 0.227$. Thus an approximate solution is obtained by replacing a_μ^p and Ψ_μ^p for these values in eq 32 to yield

$$\Psi^p = 0.496\{[\sigma + 1/(1 + 0.227\sigma)]/(1 + \rho)\} \quad (35)$$

The current function Φ (see ref 38) consists of normalizing eq 35 to that of an irreversible one-electron wave, i.e.

$$\Phi = \Psi^p/0.496 = 1 - \{[(0.227\rho)/(1 + 0.227\rho)]/(1 + \sigma)\} \quad (36)$$

Equation 36 is equivalent to eq 18 owing to $\sigma = k_3/k_1$ and $\rho = k_2C_0/k_4$.

Acknowledgment. We thank C. P. Casey for valuable help with the synthesis of IV and the National Science Foundation and the Robert A. Welch Foundation for financial support.

Registry No. I, 89044-00-8; I·K, 89044-01-9; II, 48055-09-0; III, 70083-79-3; IV, 87207-09-8; V, 87207-10-1; $Cr_2(CO)_{10}^{2-}$, 45264-01-5; $Fe_2(CO)_8^{2-}$, 25463-33-6; $Mn(CO)_4PPh_3^-$, 53418-18-1; $Cr(CO)_6$, 13007-92-6; $Fe(CO)_5$, 13463-40-6; $Mn(CO)_4(PPh_3)_2^+PF_6^-$, 70083-76-0; $Cr(CO)_5H^-$, 18716-81-9; $(\mu\text{-H})[Cr(CO)_5]_2^-$, 19571-06-3; $W(CO)_5CHO^-K^+$, 89044-02-0; $(CH_3CO)Re(CO)_4CHO^-K^+$, 89103-93-5; $Re(CO)_4BrCHO^-Li^+$, 70569-14-1; $Mo(CO)_5CHO^-K^+$, 89044-04-2; $Mn_2(CO)_9CHO^-Li^+$, 89044-05-3; $(\mu\text{-H})[W(CO)_5]_2^-$, 19773-10-5; $W(CO)_5H^-$, 77227-36-2; $(CH_3CO)Re(CO)_4H^-$, 78419-11-1; $HMn(CO)_3(PPh_3)_2$, 16972-17-1; Bu_3SnH, 688-73-3; sodiun anthracene, 12261-48-2; γ-terpinene, 99-85-4; 9,10-dihydroanthracene, 613-31-0; 1-methoxy-1,4-cyclohexadiene, 2886-59-1.

(61) Note that in the CV experiment, the first-order decay of $reCHO^{-}\cdot$ does not lead to the activation of the radical-chain process.[41]

(62) See, e.g.: Amatore, C.; Saveant, J. M. *J. Electroanal. Chem.* **1979**, *102*, 21. Matsuda, H.; Ayabe, Y. *Z. Electrochem.* **1955**, *59*, 494.